Biomimetic self-assembly of a functional asymmetrical electronic device

Mila Boncheva, David H. Gracias, Heiko O. Jacobs, and George M. Whitesides*

Department of Chemistry and Chemical Biology, Harvard University, Cambridge, MA 02138

Contributed by George M. Whitesides, December 13, 2001

This paper introduces a biomimetic strategy for the fabrication of asymmetrical, three-dimensional electronic devices modeled on the folding of a chain of polypeptide structural motifs into a globular protein. Millimeter-size polyhedra—patterned with logic devices, wires, and solder dots—were connected in a linear string by using flexible wire. On self-assembly, the string folded spontaneously into two domains: one functioned as a ring oscillator, and the other one as a shift register. This example demonstrates that biomimetic principles of design and self-organization can be applied to generate multifunctional electronic systems of complex, three-dimensional architecture.

Does biology have lessons to teach microelectronics about design and fabrication? Microelectronic devices are currently fabricated by using processes that are intrinsically two-dimensional, and the interconnectivity required in complex systems is achieved by stacking and connecting planar layers of circuits (1–3). Biological structures arise by constrained self-assembly, and are usually three-dimensional (3D) (4). We have previously demonstrated that it is possible to generate elementary 3D electrical networks by self-assembly of identical components, in a process analogous to molecular crystallization (5). The networks formed in this way have translational symmetry, and may be relevant to the design of microelectronic systems with high symmetry (e.g., memory or display); they are not appropriate for more complex systems such as microprocessors, which are asymmetrical in their structure, with different regions carrying out different functions (6). Here we report constrained self-assembly of a linear chain of structurally and functionally distinct microelectronic elements into a multidomain electronic device with asymmetrical structure and connectivity. This process is modeled on a ubiquitous biological process—the folding of a polypeptide chain into a globular protein. Our proof-of-concept demonstration of biomimetic self-assembly illustrates a strategy for fabricating 3D asymmetrical microelectronic devices. This strategy does not (yet) provide the basis for a practical method of building devices, but it does establish that concepts for the generation of 3D structure can be abstracted from biology and used to generate component-level microelectronic systems.

Protein folding is a complex process, with formation of secondary and tertiary structure proceeding at the same time (7). In the simplest description, the primary, linear amino acid sequence organizes into several secondary-structural motifs (e.g., α-helices, β-sheets), connected by short loop regions (8, 9). These secondary structural motifs fold into one or several compact domains, and form a 3D structure. In some proteins, the domains have distinct functions, e.g., membrane insertion (9), ligand binding (10), and catalysis (11). The device discussed in this work was modeled on an abstraction of a three-domain protein, formed by folding of a string of secondary structural elements. The device was built of two linear chains of 5 triangular prisms (each with a face of $\approx$5 mm), connected with a spacer; these prisms serve as analogues of secondary structural elements in proteins (Fig. 1*A*). Patterns of solder, in the form of wires and dots intended to realize electrical connections on and between the prisms, were fabricated separately by using principles of design that have been described (5) (Fig. 1 *B* and *C*), functionalized with appropriate electronic devices [complementary metal oxide semiconductor inverters and flip-flops, chip capacitor, resistors, and light-emitting diodes (LEDs)], and glued to the faces of the prisms. The solder patterns provided the information necessary for the self-assembly of the system; they were designed to give stable connections between the prisms only when all of the solder dots on the face of one prism were correctly aligned with the solder dots on the face of the next (12). We used identical pattern of solder dots for the 10 prisms. Only four of the five dots in the pattern shown in Fig. 1*B* carried specific electrical function in the system (e.g., driving voltage, ground); the additional central dot served to facilitate the correct alignment of the patterns during the assembly. All five dots of the pattern shown in Fig. 1*C* carried electrical functions (e.g., driving voltage, ground, clock signal).

Connections between the prisms in the two pentameric strings consisted of short, flexible copper wires; their lengths limited the maximum separation between adjacent prisms. The two pentamers were connected by using longer, stiffer copper wires (Fig. 1 *D* and *E*); these wires separated the two pentameric sequences during the assembly. The flexible wire linkers mimic the loop regions that connect secondary structural elements; the stiff copper wires provide an analogue of structural domains in proteins that connect the functionally important domains (e.g., the trimeric coiled-coil in hemagglutinins; ref. 13). The linear chain was suspended in an isodense aqueous solution of KBr (pH 3–4, Fig. 1*E*), and heated to a temperature above the melting point of the solder (60°C). On rotation of the vessel containing the suspended structure (approximate rotation rate, 35 rpm; ref. 14), the prisms collided under the influence of fluid shear. Capillary interactions between the drops of molten solder caused self-assembly (15, 16); these interactions are analogous to the hydrophobic interactions between secondary structural motifs in proteins (17). The positions of the rigid and the flexible connecting wires favor collisions between adjacent prisms, and guide their self-assembly. This constraint mimics the entropic restrictions imposed on the folding of proteins. The initially linear sequence folded, as designed, into an asymmetrical structure consisting of two distinct pentameric domains, one circular (C) and one linear (L), separated by the structurally rigid wire domain (S) (Fig. 1 *F* and *G*). The folding of the two pentameric domains proceeded independently. The C domain contained all of the prisms bearing inverter gates; the L domain included the prisms carrying D-type flip-flops. The solder drops, when cooled and solidified, bridged the units and provided both electrical connectivity and mechanical stability. The pattern of solder dots, together with the initial sequence and relative orientation of the prisms in each pentamer, determined the structure of each domain.

Fig. 2*A* shows the circuit diagram of the device when fully self-assembled. The inverters in the C domain formed a ring oscillator; the flip-flops in the L domain formed a shift register.

Abbreviations: 3D, three-dimensional; LED, light-emitting diode.

*To whom reprint requests should be addressed. E-mail: gwhitesides@gmwgroup.harvard.edu.

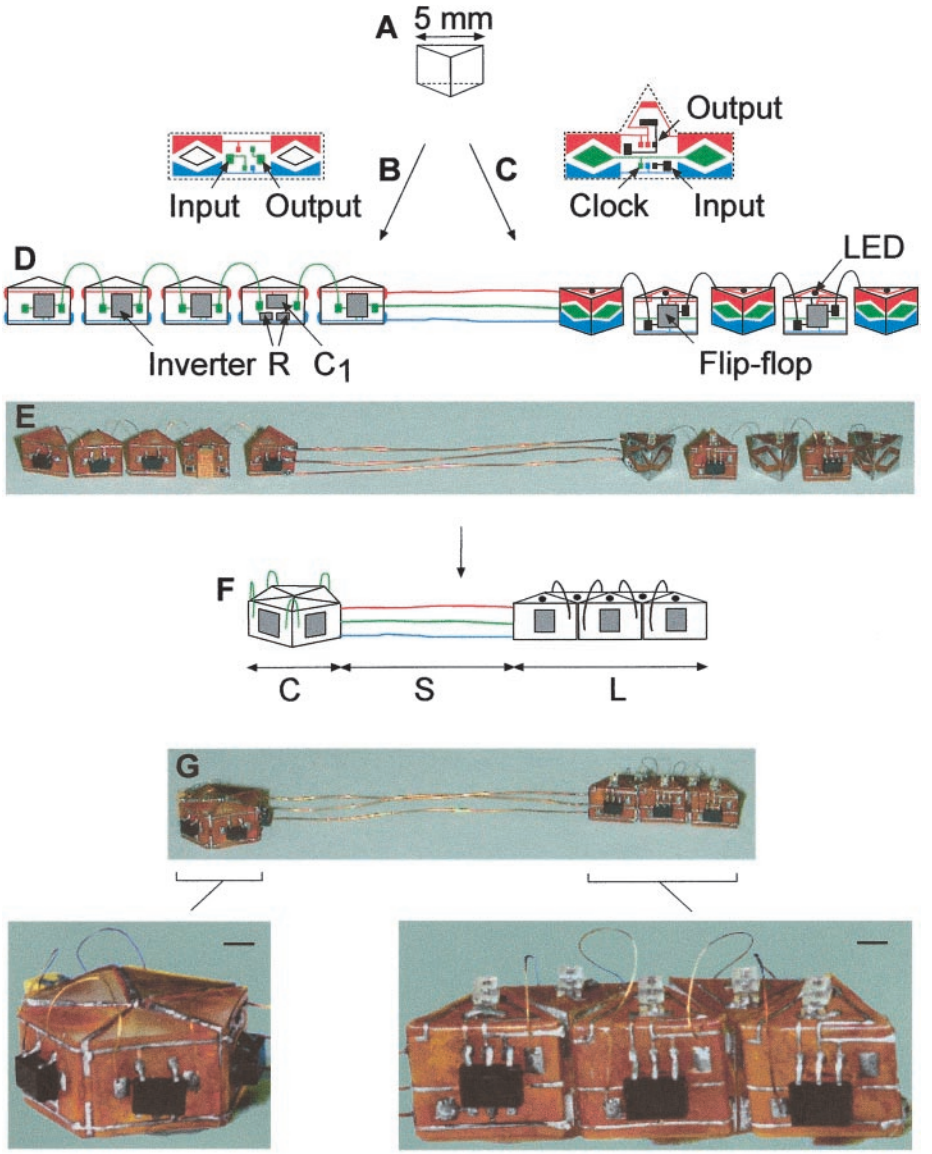

Fig. 1. Design and fabrication of the asymmetrical electronic device. (*A*) Schematic representation of a triangular prism, the basic unit in the assembly. The prisms were cast in polydimethylsiloxane (PDMS) molds using photocurable polyurethane (J-91, Summers Optical, Fort Washington, PA). (*B* and *C*) The solder pattern of contact pads, dots, and wires used for the ring oscillator and the shift register, respectively. A mirror image of the pattern shown in *C* was used on every second piece in the shift register; this pattern positioned the copper wires connecting input and output of neighboring pieces without crossing above the LEDs, for easier observation. The functions of different parts of the pattern are indicated in color: red, driving voltage; blue, ground; green, clock signal; black, data line. Single inverter gates (SN74AHC1G04, Texas Instruments, Dallas), chip resistors (R_1 = 100 kΩ, R_2 = 1 MΩ, Skywell, Walnut Creek, CA), a capacitor (C_1 = 22 μF, Skywell), D-type flip-flops (NC7SZ175, TinyLogic, Fairchild Semiconductor, South Portland, ME), and LEDs (BL-HS136, American Bright Optoelectronics, Brea, CA), all shown in gray, were soldered onto the patterns contact pads manually. The Clear input of all flip-flops was permanently kept at a High logic level, and only the D-input of the flip-flops was used. The patterns were glued onto the prisms and connected with copper linkers, as depicted in *D*. Insulated Cu wire (diameter 76 μm, length 10 mm, California Fine Wire, Grover Beach, CA) was used to connect the prisms. Thicker wire (diameter 127 μm, length 40 mm) connected the two flexible pentamers. (*E*) Photograph of the structure before folding. (*F*) Schematic drawing of the folded structure, consisting of a circular (C), structural (S), and a linear (L) domain. (*G*) Photographs of the structure after folding. (Scale bars, 1 mm.)

A ring oscillator containing only high-speed inverters would have an output frequency in the MHz range. To slow this frequency sufficiently for it to be observable by eye as changes in the LEDs states, we shifted the oscillator output down to 0.192 Hz by incorporating two chip resistors and a capacitor into the oscillator domain (18). The parallel connections between the logic elements within each domain formed during self-assembly by the fusion of solder drops; the copper wires connecting the prisms carried both the serial input/output connections within and between the domains, and the parallel connection between the domains.

After self-assembly, the device was connected to an external voltage source. Data input (D) to the flip-flops was provided by a function generator as a square wave with an amplitude +0.6 V, offset by +0.3 V, and with a frequency in the range 0.05–1 Hz. The square wave output of the ring oscillator provided a clock signal (Clk) for the shift register. Fig. 2 *B–D* illustrates the operation of the assembled, clocked shift register. Input data were transferred to the output (Q) only at the moment of Low-to-High clock transition. Because the LEDs were connected between the driving voltage and the output of each flip-flop, they reflected the changes in the output values of the

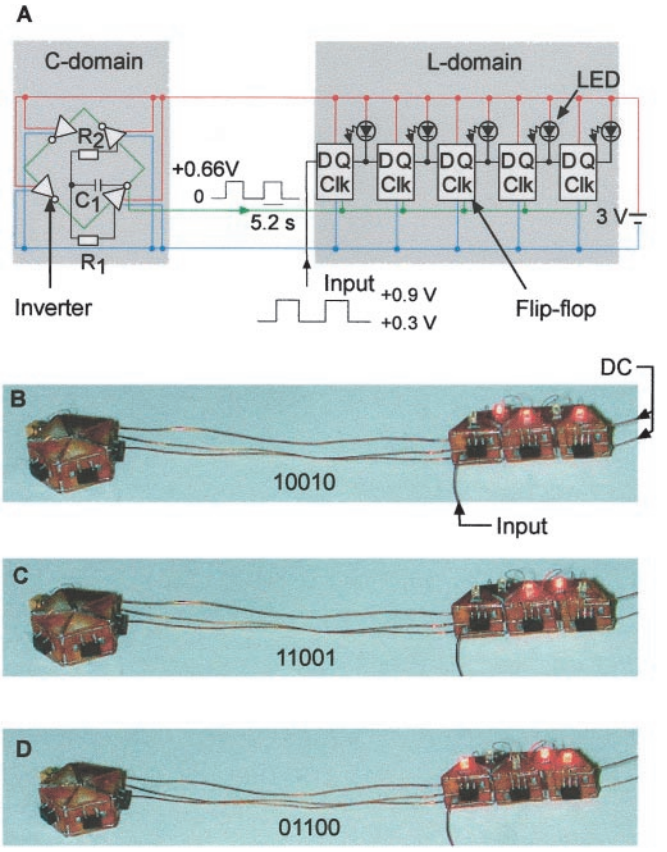

Fig. 2. Operation of the self-assembled electronic device. (*A*) Circuit diagram of the clocked shift register. The color coding of the electrical connections is as in Fig. 1. The photographs in *B–D* were taken at intervals of 5.2 s, corresponding to three consecutive clock pulses. The binary numbers stored in the shift register between the clock pulses are visualized by the LEDs, and are indicated on each photograph. Logic level 1 is coded by unlit LEDs, and logic level 0 is given by lit LEDs. The arrows in *B* indicate the connections made after the self-assembly—to an external voltage source, and to the function generator.

flip-flops. The LEDs illuminated when the output value was low, i.e., when a Low-to-High clock transition coincided with a Low (+0.3V) D input. A LED remained lit until the next Low-to-High clock transition coincided with a High (+0.9V) D input. The data input to the shift register were stored in, and shifted from left to right along, the register sequence bit by bit. As each flip-flop can store only one bit, the shift register shown here functions as a 5-bit memory device (19).

The device used in this work to illustrate the strategy of constrained, biomimetic self-assembly of an asymmetrical electronic system comprised a ring oscillator and a shift register. We chose these two elements because they are among the most important and widely used elements in microelectronic systems (20). The classes of logic elements that can be incorporated into self-assembling strings are, however, limited neither to these devices nor to the present example.

The design and assembly of the electronic device mimicked two characteristics of proteins. First, it is an asymmetrical structure that forms by constrained self-assembly from a linear precursor. Second, it localizes different functions in separate structural domains. These characteristics are common in complex proteins—immunoglobulins, integrins, cell-surface receptors, complement (4)—and are also the key elements in building complex functionality into microdevices by using this strategy. Our initial demonstration suggests many other biological mechanisms—templating (21, 22), molecular recognition (23, 24), hierarchical self-assembly (25, 26), multivalency (27)—to guide biomimetic self-assembly in microelectronic systems.

We believe that the concept of biomimetic self-assembly will be applicable to a range of complex, 3D structures. The most serious current limitation to this method is practical: we now use tedious, manual methods to fabricate the small components—appropriately modified for self-assembly and functionalized with complementary metal oxide semiconductor devices—and to connect them into linear, flexible strings. More efficient methods to fabricate the linear precursors must be developed; choosing optimum sizes and complexities for the components they incorporate are also key issues. The production of appropriate components, alone and in connected strings, will require development of new methods for parallel microfabrication. To achieve a high volumetric density of functional components in the final, self-assembled system, the components must be also smaller than those used in the present example—optimally, we believe, <10 μm—with wires of a few-micrometer diameter (28). Methods for fabricating these systems will, we suggest, begin with folding (29, 30), or self-assembly of planar components on 3D scaffolds (31). We believe that when the problem of design and fabrication of components is solved, biomimetic self-assembly will become an approach to 3D microsystems worth substantial development.

We thank J.-M. Bettex for help with photography. This work was supported by National Science Foundation Grant CHE-9901358 and a grant from the Defense Advanced Research Projects Agency.

1. Campbell, S. A. (1996) *The Science and Engineering of Microelectronic Fabrication* (Oxford Univ. Press, New York).
2. Gandghi, S. K. (1994) *VLSI Fabrication Principles* (Wiley, New York).
3. Madou, M. (1997) *Fundamentals of Microfabrication* (CRC, Boca Raton, FL).
4. Branden, C. & Tooze, J. (1999) *Introduction to Protein Structure* (Garland, New York).
5. Gracias, D. H., Tien, J., Breen, T. L., Hsu, C. & Whitesides, G. M. (2000) *Science* **289,** 1170–1172.
6. Chandrakasan, A. P., Bowhill, W. J. & Fox, F. (2001) *Design of High-Performance Microprocessor Circuits* (IEEE, New York).
7. Baker, D. (2000) *Nature (London)* **405,** 39–42.
8. Sibanda, B. L. & Thornton, J. M. (1985) *Nature (London)* **316,** 170–176.
9. Palczewski, K., Kumasaka, T., Hori, T., Behnke, C. A., Motoshima, H., Fox, B. A., LeTrong, I., Teller, D. C., Okada, T., Stenkamp, R. E., *et al.* (2000) *Science* **289,** 739–745.
10. Chothia, C., Lesk, A. M., Levitt, M., Amit, A. G., Mariuzza, R. A., Phillips, S. E. V. & Poljak, R. J. (1986) *Science* **233,** 755–758.
11. James, M. N. G., Sielecki, A. R., Brayer, G. D., Delbaere, L. T. J. & Bauer, C. A. (1980) *J. Mol. Biol.* **144,** 43–88.
12. Boehringer, K. F., Srinivasan, U. & Howe, R. T. (2001) in *Proceedings IEEE Conference on MicroElectro Mechanical Systems (MEMS)* (IEEE, Interlaken, Switzerland) pp. 369–374.
13. Bullough, P. A., Hughson, F. M., Skehel, J. J. & Wiley, D. C. (1994) *Nature (London)* **371,** 37–43.
14. Tien, J., Breen, T. L. & Whitesides, G. M. (1998) *J. Am. Chem. Soc.* **120,** 12670–12671.
15. Miller, L. F. (1969) *IBM J. Res. Dev.* **13,** 239–250.
16. Syms, R. R. A. & Yeatman, E. M. (1993) *Electronics Lett.* **29,** 662–664.
17. Bowden, N., Choi, I. S., Grzybowski, B. & Whitesides, G. M. (1999) *J. Am. Chem. Soc.* **121,** 5373–5391.
18. Horowitz, P. & Hill, W. (1989) in *The Art of Electronics* (Cambridge Univ. Press, Cambridge, U.K.), pp. 284–286.
19. Feynman, R. (1996) *Feynman Lectures on Computation* (Perseus Books, Reading, MA).
20. Kleitz, W. (1998) *Digital Electronics: A Practical Approach* (Prentice Hall, Englewood Cliffs, NJ).
21. Conn, M. M., Wintner, E. A. & Rebek, J., Jr. (1994) *Angew. Chem. Int. Ed. Engl.* **106,** 1665–1667.

22. Choi, I. S., Weck, M., Xu, B., Jeon, N. L. & Whitesides, G. M. (2000) *Langmuir* **16,** 2997–2999.
23. Paleos, C. M. & Tsiouvras, D. (1997) *Adv. Mater.* **9,** 695–710.
24. Choi, I. S., Bowden, N. & Whitesides, G. M. (1999) *J. Am. Chem. Soc.* **121,** 1754–1755.
25. Larson, S. B., Koszelak, S., Day, J., Greenwood, A., Dodds, J. A. & McPherson, A. (1993) *Nature (London)* **361,** 179–182.
26. Choi, I. S., Bowden, N. & Whitesides, G. M. (1999) *Angew. Chem. Int. Ed. Engl.* **38,** 3078–3081.
27. Mammen, M., Choi, S.-K. & Whitesides, G. M. (1998) *Angew. Chem. Int. Ed. Engl.* **37,** 2755–2794.
28. Bowden, N., Weck, M., Choi, I. & Whitesides, G. M. (2001) *Acc. Chem. Res.* **34,** 231–238.
29. Harsh, K. F., Bright, V. M. & Lee, Y. C. (1999) *Sens. Actuators A* **77,** 237–244.
30. Green, P. W., Syms, R. R. A. & Yeatman, E. M. (1995) *J. Microelectromech. Syst.* **4,** 170–176.
31. Xia, Y., Rogers, J. A., Paul, K. E. & Whitesides, G. M. (1999) *Chem. Rev.* **99,** 1823–1848.